Observation of an Adiabatic Shear Band in AISI 4340 Steel by High-Voltage Transmission Electron Microscopy

C.L. WITTMAN, M.A. MEYERS, and H.-r. PAK

Adiabatic shear bands, formed in a hollow AISI 4340 steel cylinder subjected to dynamic expansion by means of an explosive charge placed in its longitudinal axis, were characterized. The adiabatic shear bands formed in this quenched and tempered steel were of the classical "transformed" type. Scanning electron microscopy (SEM) of etched surfaces revealed that alignment of the lamellae along the direction of shear seems to be the event that precedes shear localization. The transmission electron microscopy (TEM) of a "white"-etching shear band having undergone a shear strain of approximately 4 revealed that it contained χ (Fe_5C_2) carbides in a martensitic structure. These carbides were observed to form on (112) internal microtwins. Grains could not be resolved inside of the shear band, but they could be observed in the surrounding matrix material. A traverse of the shear band was made, and there existed no definite boundary between the matrix and the shear band. No evidence of a transformation to austenite was observed. Heat transfer calculations were conducted to help explain the features observed inside of the shear band. It is concluded that the "white"-etching bands, commonly referred to in the literature as "transformed" bands, do not exhibit a transformation at values of shear strain of up to 4. The enhanced reflectivity is an etching artifact and is possibly due to microstructural changes, a very small grain size, and carbide redissolution in the bands.

I. INTRODUCTION

ALTHOUGH adiabatic shear bands have been the object of numerous studies for the past 40 years, considerable controversy exists over their structure in steels. White-etching bands have been labeled as "transformed" without irrefutable evidence for such a transformation, while dark-etching bands have been named "deformed." This paper represents an effort at identifying the structure of adiabatic shear bands in steels.

White-etching bands and layers are not restricted to adiabatic (high strain rate) deformation conditions. There are many reported cases of similar white-etching zones occurring in contact loading and frictional systems. In 1941, Trent[1] studied the formation of "martensitic" bands formed on rope wire by friction. Zener and Hollomon[2] were the first to describe that adiabatic heating effects are responsible for the formation of narrow white-etching shear bands. This landmark study was followed by numerous investigations of both a mechanical and metallurgical nature. In a number of these studies, the bands have been classified into "transformed" and "deformed," whether they etch white or dark, respectively.[3,4]

This controversy over the nature of the white-etching shear bands is due, in part, to the lack of careful observations and analyses by transmission electron microscopy (TEM). The thickness of these bands being typically of the order of a few microns, TEM is virtually the only technique available for the identification of their structure.* There are only two reports in the literature, and they both fail to identify incontrovertibly the structure of white-etching shear bands. In 1971, Glenn and Leslie[5] studied shear bands in 0.6 pct carbon steel produced by ballistic impact. The structure of the white-etching bands was difficult to resolve by TEM, because the grain size was thought to be less than 0.1 μm. The transition from the white-etching region to the matrix was gradual, with the diffraction pattern changing from a diffuse ring to a solid bct ring pattern. Glenn and Leslie[5] postulated that the white-etching region was very rapidly quenched martensite. Wingrove,[6,7] also in 1971, observed in the white-etching regions a high density of dislocations, with some cell boundaries. The microstructure was not typical of normal martensite observed in steel, yet the diffraction pattern indexed to martensite. Upon tempering of the white-etching zone, extra spots appeared in the diffraction pattern, a possible indication of carbide precipitation, although the microstructure of the white-etching region remained relatively unchanged. Small precipitates could be observed only after imaging under dark-field conditions.

The objective of this research program was to identify the microstructure of a white-etching shear band by TEM. The AISI 4340 steel in the quenched and tempered condition typically exhibits a profusion of white-etching bands when deformed at high strain rates. It was deformed at a high strain rate by a technique described in Section II.

*A recent review on adiabatic shear bands is recommended.[28]

II. EXPERIMENTAL TECHNIQUES

The medium carbon AISI 4340 sample, provided by SRI International, Menlo Park, CA, was taken from a

C.L. WITTMAN, M.A. MEYERS, and H.-r. PAK, all formerly with the Department of Metallurgical and Materials Engineering, New Mexico Institute of Mining and Technology, Socorro, NM 87801, are with Honeywell Defense Systems, Hopkins, MN 55343, the Center of Excellence for Advanced Materials, University of California at San Diego, La Jolla, CA 92093, and the Department of Metallurgy and Mineral Engineering, University of Illinois at Urbana-Champaign, Urbana, IL 61801, respectively.

Manuscript submitted July 13, 1987.

152-mm-long, 11.5-mm-thick AISI 4340 steel tube, with an outer diameter of 68.5 mm. This steel was quenched from 695 °C and then tempered at 230 °C for 2 hours, with a resulting hardness of HRC 52. The contained fragment configuration, which was used to introduce the high strain rate deformation and shear bands, is shown in Figure 1(a). This testing procedure was developed at SRI International and is described in detail in the comprehensive report by Erlich *et al.*[8] The center of the steel tube was filled with PETN (a high explosive with a detonation velocity of 7300 m/s) and packed to a density of 1.35 g/cm^3. The Chapman-Jouguet pressure of this explosive was 16.3 GPa. A 12.7-mm-thick acrylic tube was placed around the outside of the AISI 4340 steel cylinder to act as a buffer, allowing the tube to expand, creating the strain required for fragmentation. Figure 1(b) schematically shows a fragment from the cylinder containing shear bands.

Thin foil discs, 3 mm in diameter, were prepared by mechanically thinning the samples containing shear bands to a thickness of less than 30 μm. The band region was then electropolished, using a Fishione electropolishing machine (30 pct Nital at −20 °C) by masking the area around the shear band on one side of the disc with "stop-off" lacquer. This, in effect, concentrated the polishing on the shear band region. This procedure was necessary, because the shear band resisted all attempts to thin it using any other means. This produced a hole in the region near the shear band, but the transparent area was not directly on the shear band. Therefore, ion milling, using a "cold finger," was used to widen this hole and, at the same time, thin the area around the shear band. The ion milling was not thought to do any damage to the microstructure since it had already been shock loaded by the deformation process. The foil was then observed in a Kratos 1500 transmission electron microscope, located at the Lawrence Berkeley Laboratory in Berkeley, CA, operated at 1.5 MeV.

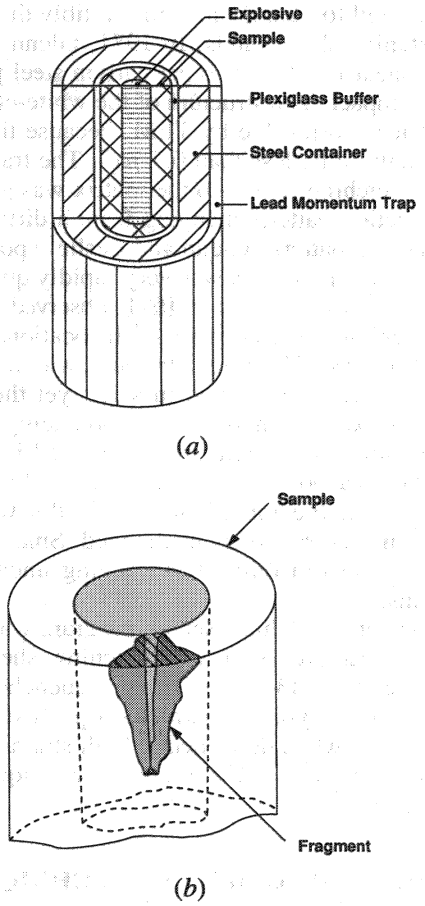

Fig. 1—(*a*) Contained fragment configuration used in SRI International experiments and (*b*) sketch of fragment cross section.

III. RESULTS AND DISCUSSION

A. *Optical and Scanning Electron Microscopy*

All of the bands observed in the fragment were of the white-etching type. A typical cross section consisted of two long bands, as shown in Figure 2. The bands in this cross section were traversed by spall cracks, which are a result of the reflected shock wave creating a tensile pulse. Thus, the shear band is formed in this area, prior to spalling, since the spall passes directly through the shear band, which continues on into the sample. This spall is near the center of the fragment, and it is thought that it was produced from the reflection of the shock wave at the outer surface of the sample tube. This reflected release wave collided with the tail portion of the original shock wave, creating the tensile pulse. From the speed of sound for steel (3500 m/s) and the width of the tube (11.5 mm), this reflection was estimated to occur 4.9 ms after the deformation had initiated. Thus,

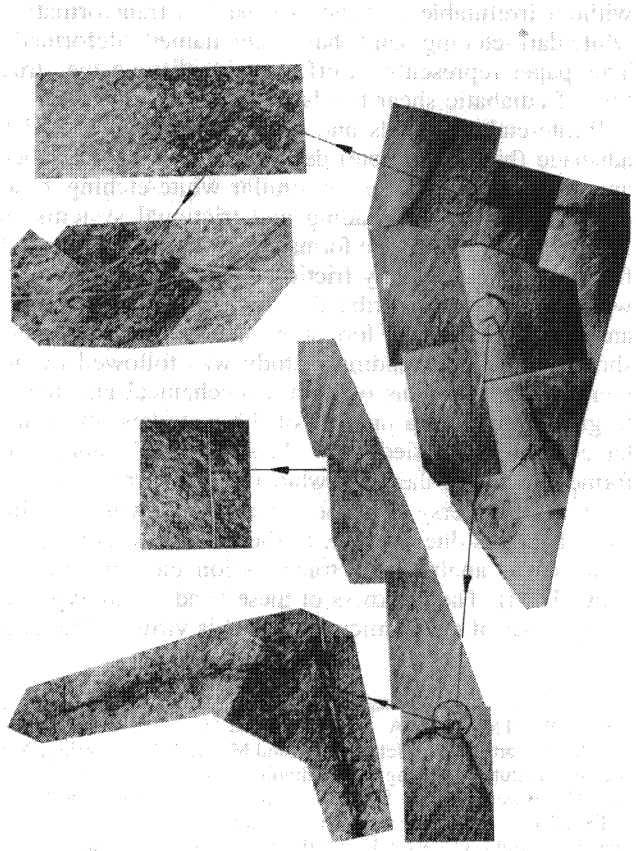

Fig. 2—Cross section of the fragment. Circled areas are reproduced at higher magnifications for greater detail; arrows point to the higher magnification views.

the shear band in this area would have formed some time prior to 4.9 ms after deformation had begun.

The microstructure within the band is very hard to elucidate using optical microscopy (Figure 2). Yet it is possible to observe the large amount of deformation associated with the shear band using scanning electron microscopy (SEM) of the etched surface (Figure 3). The martensite laths characteristic of the quenched and tempered material seem to be absent from the interior of the band, and the edge of the band does not have a uniform boundary with the matrix. The surrounding material in the matrix has been highly deformed plastically. Other features which may be observed in this image are the small incipient (not yet fully formed) bands associated with the larger shear band, indicated by the arrows in Figure 3. They are about 0.5-μm wide and travel 30 to 50 deg to the band, eventually joining it. These will be discussed further in this section.

The band often contained voids and smaller microcracks (Figure 4). These spherical voids are thought to have been produced from tensile stresses acting within the band. The band, being at very high temperature and therefore ductile, deforms readily in tension by void nucleation and growth. Material within the band has, by virtue of the higher temperature, a lower flow stress than the matrix. The crack in this figure has a somewhat sharp tip, which is indicative of a brittle-type fracture, and is thought to have occurred after the band had formed and cooled considerably.

Near the tip of the shear bands, these voids and microcracks were less prominent. Generally, the tip of the shear band consisted of a highly deformed region, narrower than the fully developed band. This observation of the band generally widening from the tip toward the tail was common to all of the bands observed. The average final width of the shear bands in the AISI 4340 steel was 13.5 μm. It should be realized that these measurements were not done on a surface exactly perpendicular to the plane of the band. The length of the band which preceded this width (distance to the tip) was 180 μm. At the tip (Figure 5(a)), the material flow was less prominent, and the white etching gradually disappears. At increasing distance from the tip (along the band length), the traces of plastic flow increased gradually. Figure 5(b) shows the extremity of a band where bifurcation occurred. Bifurcation is observed commonly in cracking, and the same energetics should govern it under shear and tension. These observations lend credence to the theory of Curran[9] that shear bands nucleate and grow and to the various attempts at modeling shear band as mode II cracks[10,11] propagating through a material. The effect of the plastic response of a material on the development of the plastic deformation region ahead of a shear band has recently been modeled by Kuriyama and Meyers[12] and by Curran and Seaman.[13]

The minimum propagation velocity of the shear band tip was estimated. A minimum band tip velocity may be obtained by dividing the time for band formation by the total length of the band. Using as a basis the observation that spalling had fractured the shear band in 4.9 ms, the velocity for growth of the band was estimated by dividing the total measured length of the band of 10.2 mm

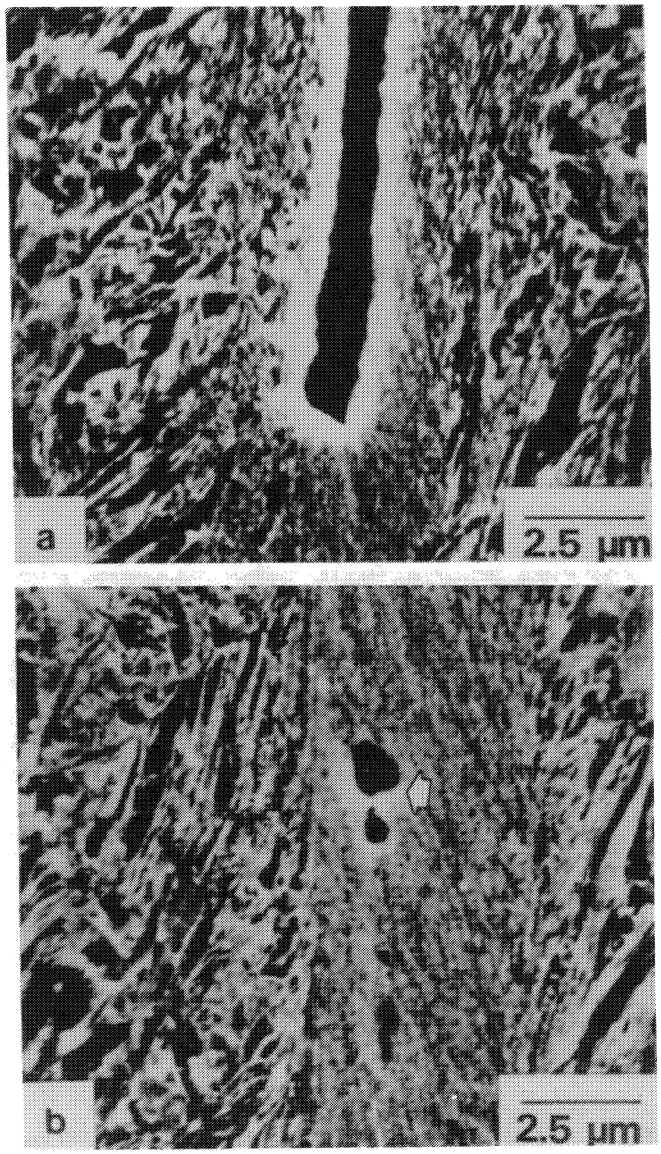

Fig. 4—Scanning electron micrographs of defects inside of a shear band in AISI 4340 steel: (*a*) blunt crack and (*b*) voids.

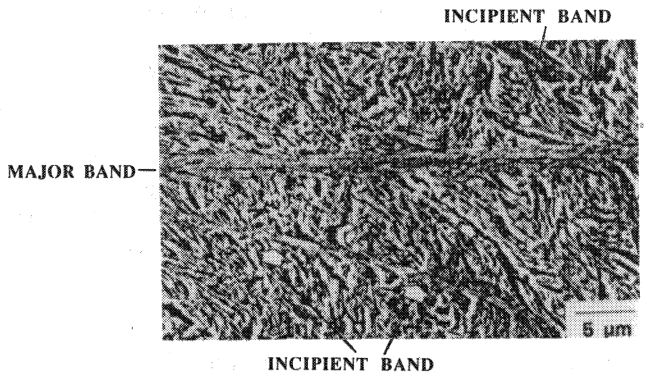

Fig. 3—Scanning electron micrograph of polished and etched section of a shear band in AISI 4340 quenched and tempered steel. Note that the boundary between the band and matrix is not well defined, as well as the presence of microbands.

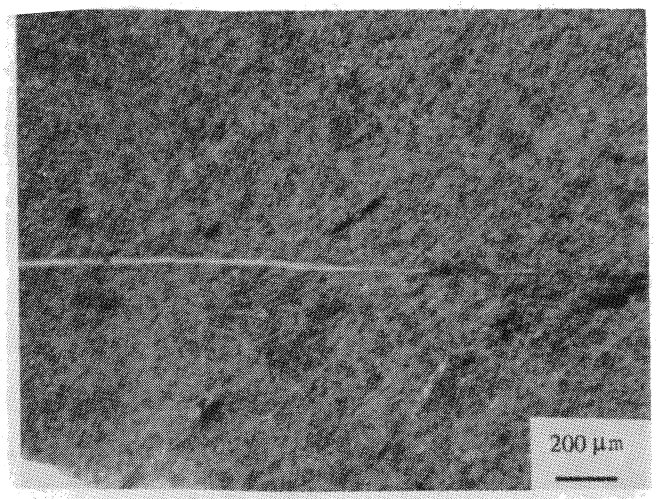

(*a*)

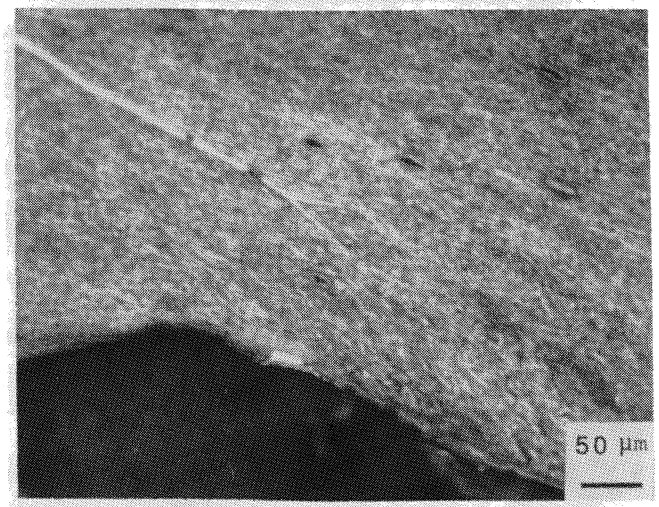

(*b*)

Fig. 5—(*a*) Optical micrograph of shear band tip in AISI 4340 steel and (*b*) shear band tip at which bifurcation occurred.

by the time; the resulting value is 2100 m/s. To approximate the strain rate of the band, the microstructure was etched to reveal previous austenitic grain boundaries. From these, the relative displacement of the band material was found. A displacement of 9.8 μm was measured in a region where the band was 2.5-μm wide. The ratio of these two numbers is the shear strain and was found to be 3.92; it was applied in a maximum time of 4.9 ms, giving rise to a minimum strain rate of $0.80 \times 10^6\ s^{-1}$. This is indeed a very high strain rate. Much higher strains (as high as 572 in the shear band) have been observed by Moss,[14] and therefore, the estimated strain in the shear band is fairly low. The temperature rise in the shear band and the associated microstructural changes are dependent on the strain. A recent report of the austenitic phase in a shear band in a similar steel is described by Meunier *et al.*[15]

Microhardness traverses were made perpendicular to the length of the band, and the average of five readings is plotted in Figure 6. The maximum and minimum readings are indicated by the error bars. The large amount

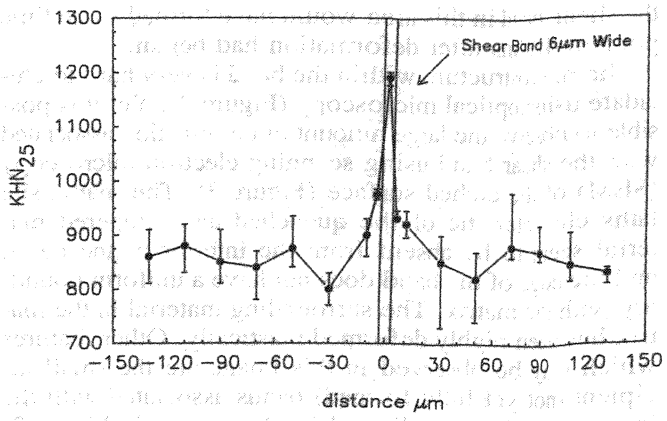

Fig. 6—Microhardness of the shear band in AISI 4340 steel.

of error in the readings may be attributed to the fact that a small load was used. This was required to keep the size of the indentation below the width of the shear band. No thermal softening was observed in these traverses, although Rogers and Shastry[16] observed softening in the regions adjoining the shear band. The average hardness value of KHN 1195 in the shear band is similar to that expected in quenched AISI 4340 microstructures. It also is the hardness expected of heavily deformed, quenched, and tempered AISI 4340 steel.

The sample was also tested after being immersed in liquid nitrogen for 1 hour. This would transform any possible austenite to martensite. The hardness measurement of the band remained unchanged, as did the observed microstructure in the optical microscope. Thus, no evidence of austenite in the band was produced by this test.

B. *Transmission Electron Microscopy*

The objective of the TEM was to identify the microstructure present in a white-etching shear band. To accomplish this, high-voltage electron microscopy was used to achieve the required foil penetration, ensuring that the shear band would be observed. All the transmission electron micrographs presented were taken at an operating voltage of 1.5 MeV. The foil thickness of the samples observed was at least two grains thick and possibly five. Thus, the imaging condition in all of the micrographs was dynamical.

A feature which was observed in the proximity of the band was incipient band formation. Several such regions were observed in the scanning electron microscope, as indicated by the arrows in Figure 3. These bands consist of highly deformed martensitic plates (Figure 7) which show alignment along the direction of material flow. The regions of more pronounced flow are marked by arrows on the small sketch.

A traverse of the shear band is very much different from the observation of the incipient band (Figure 8). A boundary in this figure has been drawn to indicate the transition between the matrix and the shear band. As may be seen, this is arbitrary since no obvious transition between the matrix and the shear band may be observed. This is in contrast to what is observed in titanium and

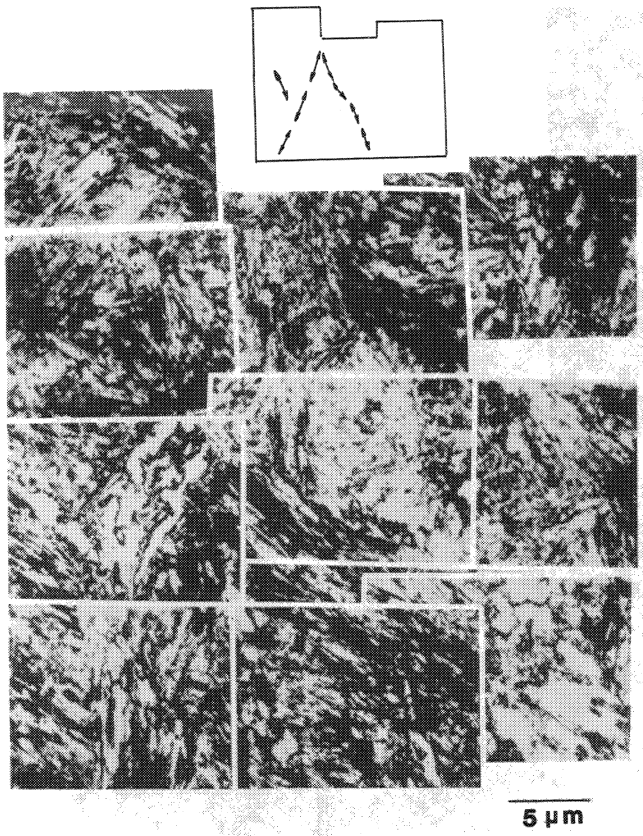

Fig. 7—Transmission electron micrograph of incipient band formation in AISI 4340 steel.

titanium alloy,[17] where a very definite boundary is observed between the shear band and the matrix. It is, however, consistent with the observations in the optical and scanning electron microscope.

In the center of the shear band, no grain boundaries could be resolved. This is due, in part, to the interference produced by the large foil thicknesses of up to five grains thick. As a result, a large number of Moiré fringes were observed in the sample (Figure 9). Indexing the electron diffraction pattern from this region revealed

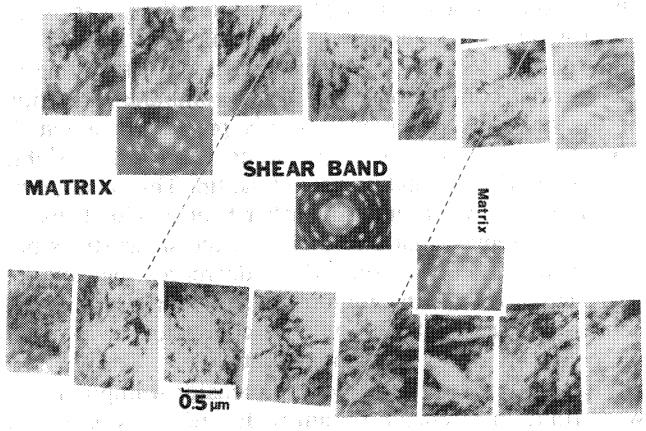

Fig. 8—Overall view of a shear band; two traverses of the shear band region are presented.

that the microstructure contained both martensite and X carbides.[18] The results of the indexing for each of the three diffraction patterns are presented in Table I. These carbides occur in the transition from the epsilon to the omega carbide in the early portion of third-stage tempering. The unique feature about their presence in the shear band is that they require a considerable amount of time to form. In the temperature range of 200 °C to 400 °C, this time is at least 20 minutes.[19]

To resolve the features in the shear band, dark-field microscopy was used. Figure 10 shows a bright-field image and two corresponding dark-field images. Figure 10(b) was produced using the 111_{χ} carbide reflection and 10(c) was produced using the $211_{\alpha'}$ martensite reflection. Using trace analysis, the carbides revealed in Figure 10(b) are located on (112)-type internal twin boundaries. These internal boundaries are common in martensite, even before the shock loading, and carbides of the Fe_3C type are known to nucleate and grow on the internal boundaries.[20,21] Thus, the Hagg carbides are expected in this location as precursors to the Fe_3C cementite carbide. As may be observed, the carbides are 5 to 150 nm in thickness and formed as films on the internal twin boundaries. Figure 10(c) images α'-martensite either above or below the grain containing the carbides.

Toward the boundary between the matrix and the shear band, cementite carbides were observed (Figure 11). These carbides have a diameter varying between 5 and 200 nm, determined from the dark-field micrograph (Figure 11(b)). They were observed to be independent of the internal twinning. This cementite could be distinguished from the carbides by the clear difference in the diffraction pattern.

The occurrence of the tweed microstructure in many of the images (Figure 12) leads to the belief that there was a significant amount of carbon in solution.[22] This tweed structure is associated with heavily deformed martensites in which the carbon is tied up at dislocations, creating an imaging effect from interference of the electron beam and these carbon atoms located at dislocations. The result is a tweedlike imaging structure, typically seen in Figure 12. The matrix material, on the other hand, exhibited the characteristic martensite lath structure. Figure 13 shows the substructure of an AISI 4340 specimen (undeformed) having undergone the same heat treatment as the quenched and tempered specimen.

The presence of Hagg carbides and cementite carbides in the microstructure may occur from one of two possibilities. The first is that the material in the shear band has been transformed to austenite, rapidly quenched to martensite, and then the remaining adiabatic heat due to the shearing reforms the carbides. This tempering may be aided by the residual heat of the deformation process which requires longer times to dissipate. The second possibility is that the carbides are those of the matrix and have not reformed. The likelihood of the latter hypothesis is supported by the fact that it requires a relatively large amount of heat to form these carbides in the matrix. Another supportive piece of evidence is that there were absolutely no traces of austenite in the material. In splat quenching operations from the austenitic phase, the presence of austenite is very common.[23] Thus, it is very unlikely that there was a transformation of the shear band

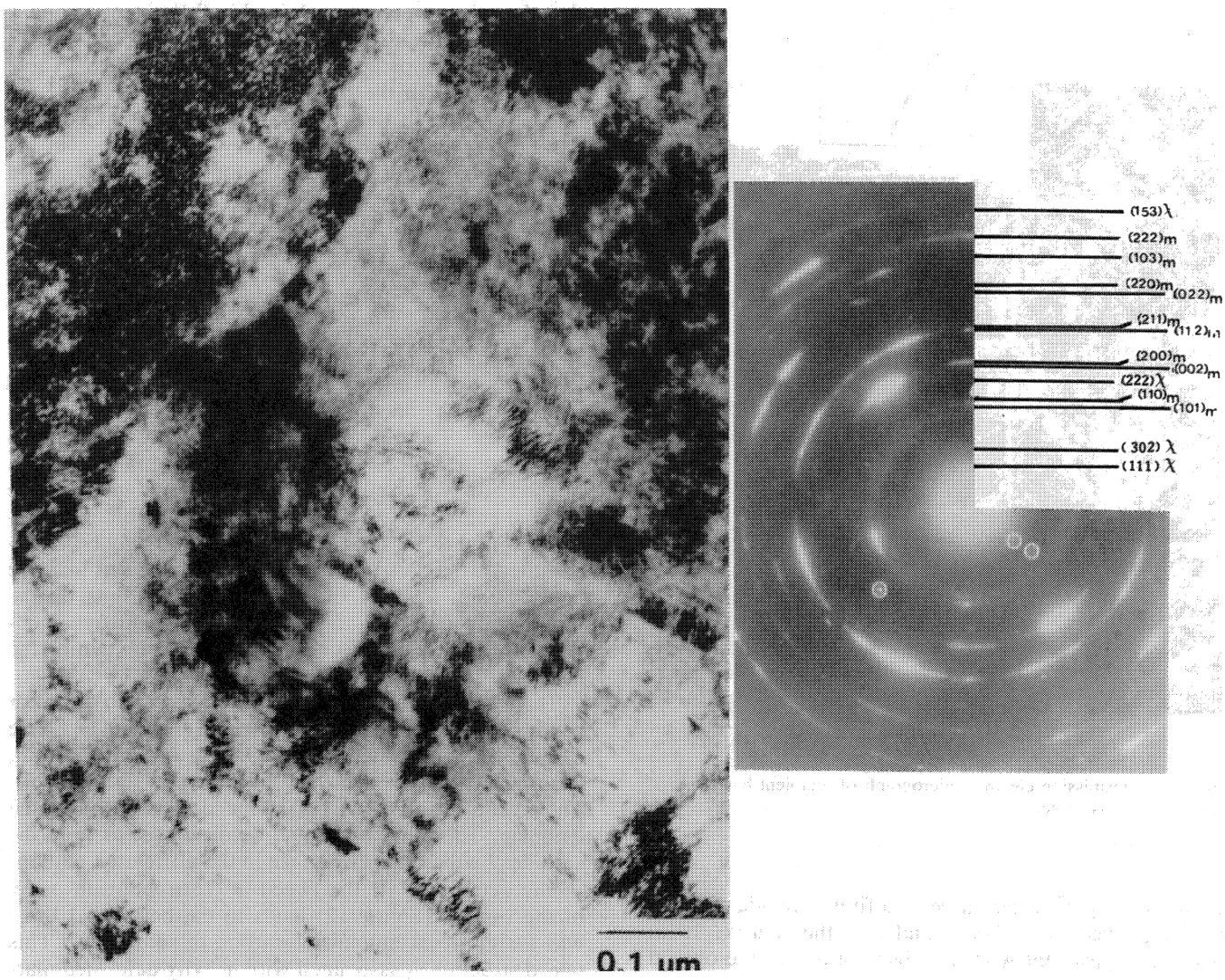

Fig. 9—Indexed pattern of the shear band region with image of this region.

material to austenite and subsequent quenching to martensite. This point will be discussed in further detail in the thermal model of Section III–C.

C. *Heat Flow Model*

To aid in the explanation of the microstructures observed, a finite-difference model was used to describe the thermal history of the shear band. Any thermal model which attempts to approximate the temperature of a shear band starts with addition of heat into the deforming region and then allows the bulk material to quench the heat-affected zone (HAZ). Two mathematically tractable methods for placing the heat into the band were used: the first is to instantaneously place a hot zone of the given thickness into the band and allow it to cool; the second method places heat into the band from its center at a constant rate, until the temperature at some distance away from the center reaches a predetermined temperature, after which heat is no longer added and the region is allowed to cool. The first method is described by Carslaw and Jaeger,[24] who present a general solution for a semi-infinite slab in which heat is fed into the free surface so that a layer of specified thickness reaches a temperature, while the rest of the material is at the reference temperature. At time $t = 0$, heat is allowed to flow from the layer to the bulk. The second method was chosen since it accounts for the fact that the shear bands do grow and then stabilize at some thickness. Thus, the material on the outside of the band is preheated due to the thermal conduction prior to the complete formation of the band. A schematic of this process is given in Figure 14. The band is propagating from left to right, and the HAZ is expanding behind the tip. This then grows to some final width and no further heat is added, using the basic premise that a lowering of the shear stress occurs in the heated region, which decreases the amount of plastic work in the region. Heat is deposited at the center, and the heat may only be conducted away from the center by one-dimensional heat flow.

The program used was a one-dimensional implicit forward finite-difference program with time steps of 4.2 ns and a node spacing of 0.2 μm. The band width of interest is 8.0 μm. Some considerations which must be

Table I. Diffraction Pattern Interpretation of the Matrix/Band Boundary Region

Measured d Value	α'-Martensite	Fe_5C_2	Fe_3C	Ferrite
	Calculated d Spacings in nm and Respective Reflecting Plane			
0.389	—	0.381 (300)	0.376 (101)	—
0.3195	—	0.316 (111)	0.3025 (111)	—
0.225	—	0.229 (120)	0.219 (201)	—
0.1934	0.2019 (110) (101)	0.1921 (221)	0.197 (112)	—
0.1640	—	0.1649 (122)	0.164 (212)	—
0.1350	—	0.134 (023)	0.135 (232)	—
0.1189	0.1797 (112)	0.1186 (114)	0.119 (250)	0.1170 (211)
0.1095	0.1028 (202)	0.1095 (404)	0.1098 (143)	0.101 (220)
0.0954	—	0.0956 (134)	0.0953 (521)	—
0.849	—	0.0848 (144)	0.08471 (215)	—
	Diffraction Pattern Interpretation of the Matrix Region			
0.365	—	0.381 (300)	0.376 (011)	—
0.245	—	0.242 (311)	0.238 (121)	—
0.1927	0.201 (110)	0.1921 (221)	0.1974 (112)	—
0.1636	—	0.1640 (421)	0.1641 (212)	—
0.1341	—	0.1341 (331)	0.1343 (241)	—
0.1110	0.116 (121)	0.110 (224)	0.117 (014)	—
0.1099	0.1009 (220)	0.1044 (024)	0.1094 (143)	0.101 (220)
0.0953	0.091 (103)	0.0956 (134)	0.0952 (521)	—
0.0770	0.0772 (213)	—	—	—
0.713	0.0714 (040)	—	—	—
Measured d Value	α'-Martensite	Fe_5C_2	Fe_3C	γ-Austenite
	Diffraction Pattern Interpretation of the Quenched Material			
0.3164	—	0.3164 (111)	—	—
0.215	0.203 (101)	0.212 (220)	0.214 (012)	0.205 (111)
0.176	—	0.177 (402)	0.176 (122)	0.176 (200)
0.125	0.117 (112)	0.125 (004)	0.125 (410)	0.126 (220)
0.101	0.101 (202)	0.101 (024)	0.101 (034)	0.103 (222)
0.0882	0.0930 (310)	0.0881 (355)	0.885 (115)	0.895 (400)

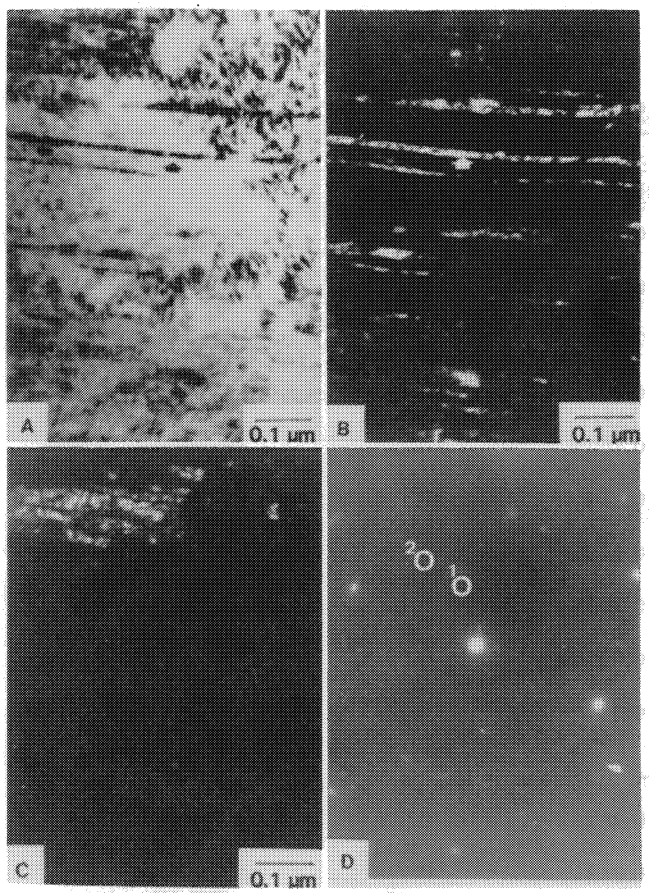

Fig. 10—(*a*) Bright-field and (*b*) and (*c*) dark-field micrographs indicating the presence of *X* carbides in the shear band on 112 internal twins. Image (b) is from the circled spot 1, 111_{χ} and image (c) from the circled spot 2, $211_{\alpha'}$ in (*d*).

accounted for in the model are that: thermal diffusivity in the program is assumed to be independent of temperature (8.1×10^{-6} m^2/s); heat was no longer added when the temperature 4 μm from the center was 90 pct of the temperature at the center of the shear band; the

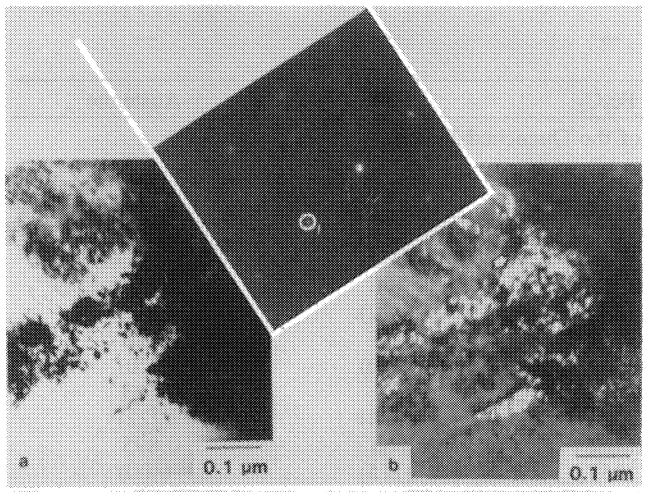

Fig. 11—Evidence of cementite carbides near the boundary between the shear band and the matrix: (*a*) bright-field image and (*b*) dark-field image of spot 1.

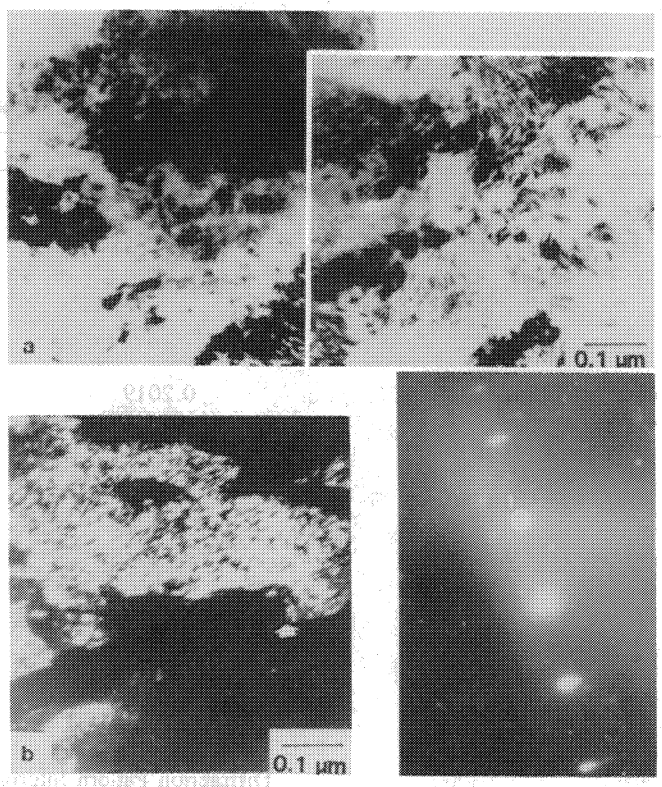

Fig. 12—Tweed microstructure of the shear band region: (*a*) bright-field image and (*b*) dark-field image of spot 1.

medium is assumed to be semi-infinite; heat effects due to shock wave propagation in the material are not accounted for; no nonuniform heat flow is considered. The temperature rise of 800 °C was selected, since this is well above the A1 line of the iron-carbon phase diagram, and it is a reasonable temperature rise from the observed strains and strain rates applied to the AISI 4340 sample. Temperature rises of 500 °C, 600 °C, 700 °C, 900 °C, and 1000 °C were also calculated with similar results and cooling rates.

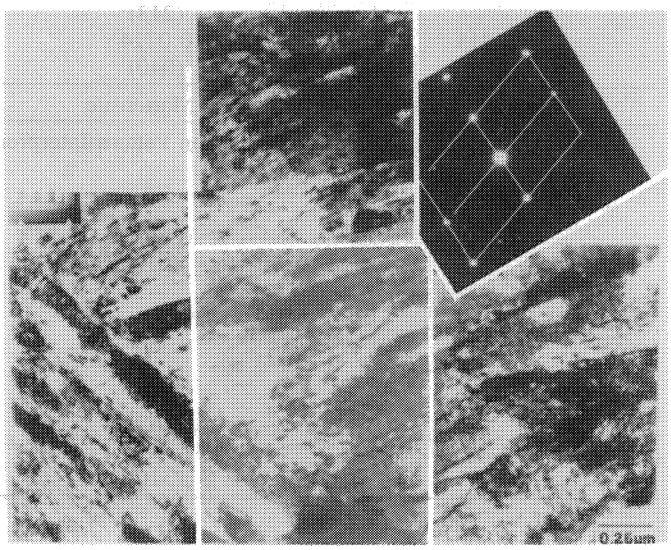

Fig. 13—Undeformed AISI 4340 steel showing the lath structure.

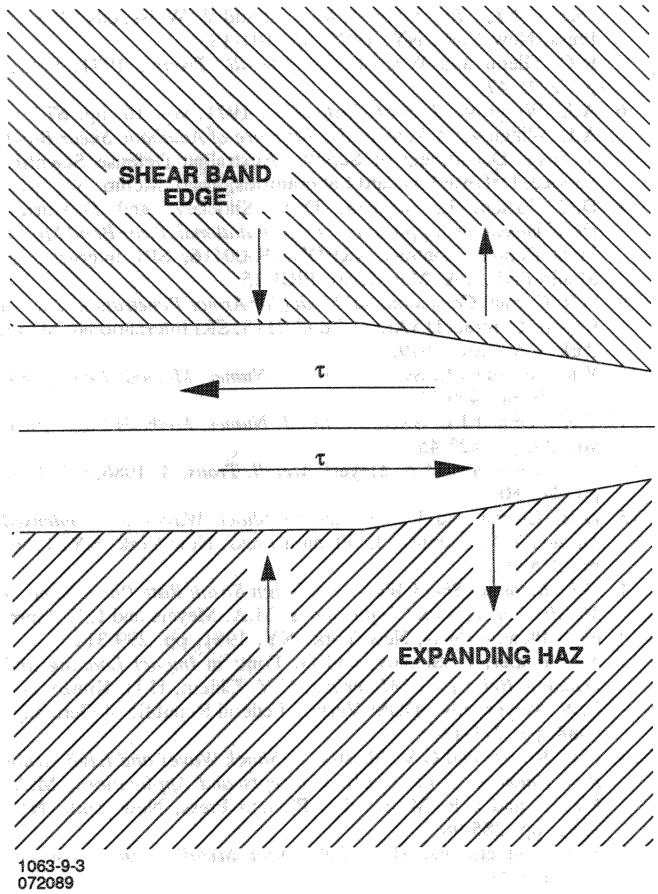

Fig. 14—Schematic of the placement of heat into the shear band.

Figure 15 shows the temperature-distance profiles at selected times during the heating and cooling process. It can be seen that the band was cooled in less than 1 ms. The cooling curve (temperature *vs* time) for the center of the shear band is shown in Figure 16. The resulting mean cooling rate is approximately 10^6 s^{-1}. This is similar to those which are observed in splat quenching. The less realistic calculation using Carslaw and Jaeger[24] predicts a time of 2 μs for cooling to one-half of the maximum temperature (in Kelvins). Considering that the predicted cooling rates are high, if the material was

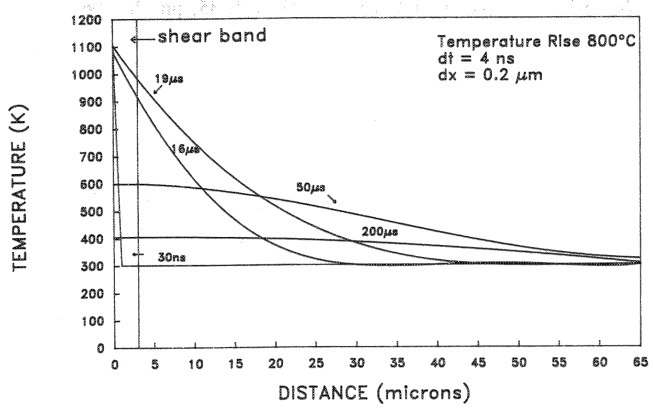

Fig. 15—Thermal profiles at various times for heat flow from a shear band.

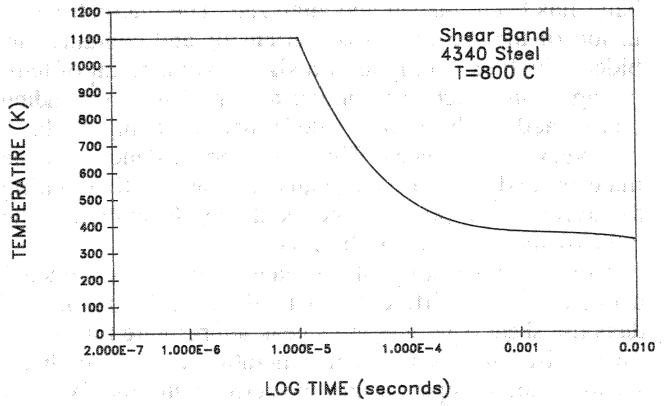

Fig. 16—Cooling curve for the center of the shear band.

transformed to austenite, retained austenite should be present in the band. Ruhl and Cohen[25] observed that by splat quenching carbon steels, the amount of retained austenite was similar to that found in conventionally quenched steels. This was dependent on the temperature from which the sample was quenched. For example, if the material was, in fact, quenched from an austenitic phase, retained austenite is expected to be found. The TEM observations do not show this to be the case, as does the fact that when the sample was supercooled into liquid nitrogen, no change in hardness occurred. Yet the amount of shear observed is sufficient to produce a temperature rise in the band area to the austenitic regime, according to the various theories for converting the plastic work into heat.

One possible explanation is that the heat was not present in the band for a long enough period of time for the up-quench transformation to austenite to have occurred.[27] Without this initial transformation, the transformation to martensite could not have occurred. The thermal model does indicate that there was enough time for carbon diffusion to have occurred. Therefore, it is proposed that the hardening of the band region is due, in part, to carbon diffusion, with the aid of the adiabatic heat, to dislocation sites within the heavily deformed martensitic shear band. This would then reduce the carbide particle size, as observed in the shear band martensite. It would also explain the thermal softening which was observed in many microhardness traverses by Rogers and Shastry,[16] although not in the present study. This also lends credence to the theory that, inside the band, carbides are broken down and redissolved, pinning dislocations.

IV. CONCLUSIONS

This study has determined the microstructure of an adiabatic shear band in AISI 4340 steel formed at a minimum strain rate of 0.8×10^6 s^{-1} and with an accumulated shear strain of 3.92 using the transmission electron microscope. While previous workers have done this, they could not determine the location of carbon and carbides in such a band nor did they observe the transition from the matrix to the band. The present work does exactly that; the entire region surrounding the shear

band has been imaged and analyzed. The microstructure inside of the shear band is martensitic and contains carbides which exist only after a significant amount of tempering. This structure is similar to that of the surrounding matrix and has been highly deformed, breaking the laths into very small pieces. There was no evidence that the material had transformed to austenite at any time during the deformation process. Incipient band formation in the bulk material was also observed.

The thermal history of the band region was modeled using the finite difference method; the calculation predicts the shear band was at its peak temperature for 19 μs. The entire process for heat generation due to adiabatic shearing and dissipation into the surrounding matrix takes less than 200 μs.

The general conclusion from the thermal history and the TEM observations is that the observed white etching of this region is an artifact of the etching. The white etching is not a particular indication of a phase transformation; it indicates that carbides have been dissolved or are too small to produce localized pitting, which would result in a darkened etching; an alternative explanation is that the microcrystalline structure inside the band changes the etching characteristics.

ACKNOWLEDGMENTS

The authors would like to express their appreciation to Dr. D.A. Shockey and Mr. D.C. Erlich of SRI International for the AISI 4340 steel fragment. The TEM was performed at the National Center for Electron Microscopy, Lawrence Berkeley Laboratory, Berkeley, CA. This research was funded by the Department of Economic Development and Tourism of New Mexico through the Center for Explosives Technology Research. The support by the University Research Initiative (URI) Center for Dynamic Performance of Materials in the latter stages of this investigation is gratefully acknowledged. The authors also thank the reviewer for his careful attention to this manuscript.

REFERENCES

1. E.M. Trent: *J. Iron Steel Inst.*, 1941, vol. 143, pp. 401-12.
2. C. Zener and H.H. Hollomon: *J. Appl. Phys.*, 1944, vol. 9, pp. 22-32.
3. H.C. Rogers: *Annu. Rev. Mater. Sci.*, 1979, vol. 9, pp. 283-311.
4. H.C. Rogers: in *Material Behavior Under High Stress and Ultrahigh Loading Rates*, J. Mescall and V. Weiss, eds., Plenum Press, New York, NY, 1983, pp. 101-18.
5. R.C. Glenn and W.C. Leslie: *Metall. Trans.*, 1971, vol. 2, pp. 2945-47.
6. A.L. Wingrove: *J. Aust. Inst. Met.*, 1971, vol. 16, pp. 67-70.
7. A.L. Wingrove: *A Note on the Structure of Adiabatic Shear Bands in Steel*, Department of Supply, Australian Defense Scientific Service, Defense Standard Laboratories, Tech. Memo. 33, 1971.
8. D.C. Erlich, L. Seaman, D.A. Shockey, and D. Curran: *Development and Application of Computational Shear Band Model*, Final Report, Contract ARBDL-CR-00416, SRI International, Menlo Park, CA, Mar. 1980, PRB-15.
9. D.R. Curran: *Computational Model for Armor Penetration*, Annual Report, Contract DAAK 11-78-C-0115, SRI International, Menlo Park, CA, Nov. 1979.
10. Y.K. Lee and J.L. Swedlow: *Int. J. Numer. Methods Eng.*, 1984, vol. 20, pp. 409-21.
11. Y.K. Lee and J.L. Swedlow: *Int. J. Numer. Methods Eng.*, 1984, vol. 20, pp. 423-45.
12. S. Kuriyama and M.A. Meyers: *Metall. Trans. A*, 1986, vol. 17A, pp. 443-50.
13. D.R. Curran and L. Seaman: in *Shock Waves in Condensed Matter*, Y.M. Gupta, ed., Plenum Press, New York, NY, 1986, pp. 315-20.
14. G.L. Moss: in *Shock Waves and High Strain Rate Phenomena in Metals: Concepts and Applications*, M.A. Meyers and L.E. Murr, eds., Plenum Press, New York, NY, 1981, pp. 299-312.
15. Y. Meunier, L. Sangoy, and G. Pont: in *Impact Loading and Dynamic Behavior of Materials*, C.Y. Chiem, H.D. Kunze, and L.W. Meyer, eds., DGM Verlag, Federal Republic of Germany, 1988, pp. 711-18.
16. H.C. Rogers and C.V. Shastry: in *Shock Waves and High Strain Rate Phenomena in Metals: Concepts and Applications*, M.A. Meyers and L.E. Murr, eds., Plenum Press, New York, NY, 1981, pp. 285-98.
17. M.A. Meyers and H.-r. Pak: *Acta Metall.*, 1986, vol. 34, pp. 2493-99.
18. K.H. Jack and S. Wild: *Nature (London)*, 1966, vol. 212, pp. 248-50.
19. F.E. Werner, B.L. Averbach, and M. Cohen: *Trans. ASM*, 1956, vol. 49, pp. 823-41.
20. Y. Ohmori and S. Sagusava: *Trans. Jpn. Inst. Met.*, 1971, vol. 12, p. 170.
21. Y. Ohmori: *Trans. Jpn. Inst. Met.*, 1972, vol. 13, p. 119.
22. P.J. Fullingham, H.J. Leary, and L.E. Turner: in *Electron Microscopy and Structure of Metals*, G. Thomas, ed., University of California Press, Berkeley, CA, 1972, pp. 163-72.
23. G.Y. Lai, W.E. Wood, R.A. Clark, V.F. Zackay, and E.R. Parker: *Metall. Trans.*, 1974, vol. 5, pp. 1663-70.
24. H.S. Carslaw and J.C. Jaeger: *Conduction of Heat in Solids*, 2nd ed., Clarendon Press, Oxford, 1959, pp. 54-57.
25. R.C. Ruhl and M. Cohen: *Trans. AIME*, 1969, vol. 245, pp. 241-45.
26. S.J. Donachie and G.S. Ansell: *Metall. Trans. A*, 1975, vol. 6A, pp. 1863-75.
27. G.R. Speich and A. Szirmae: *Trans. AIME*, 1968, vol. 245, pp. 1063-74.
28. S.P. Timothy: *Acta Metall.*, 1987, vol. 35, pp. 301-06.